Journal of Inflammation Research

Dovepress
Taylor & Francis Group

Open Access Full Text Article

ORIGINAL RESEARCH

Time-Course Renal and Pulmonary Injury Analysis and Bioinformatics Screening of Core Pathogenic Genes and Immune Cell Infiltration Patterns in a Sepsis

Anwaier Apizi*, Jian Li*, Paiheriding Kamilijiang, Chun-Bo Yang, Zheng-Kai Wang, Rui-Feng Chai, Zhao-Xia Yu

Department of Intensive Care Unit, The First Affiliated Hospital of Xinjiang Medical University, Urumqi, 830054, People's Republic of China

*These authors contributed equally to this work

Correspondence: Zhao-Xia Yu; Rui-Feng Chai, Department of Intensive Care Unit, The First Affiliated Hospital of Xinjiang Medical University, Urumqi, 830054, People's Republic of China, Tel +86 13899858397; +86 13999819217, Email zhaoxia_yu01@126.com; chairuifeng_chai@126.com

Objective: This study aimed to evaluate the extent of organ damage associated with sepsis and to identify key genes implicated in its pathogenesis.

Methods: Eighteen rats were randomized into experimental and control groups. Cecal ligation and puncture induced sepsis in the experimental group, with lung and kidney inflammatory injury assessed at 12, 24, and 36 hours. Gene expression profiles of sepsis patients and healthy controls were obtained from Gene Expression Omnibus database. Weighted gene co-expression network analysis and bioinformatics identified sepsis-related pathways and core genes, constructing a predictive risk model. Immune cell composition was compared between groups, and correlations between core gene expression and immune cell populations were analyzed.

Results: The experimental group exhibited greater lung and kidney tissue damage at all time points compared to the control group, with severity increasing over time. Cross-analysis identified 505 core genes associated with sepsis. Gene Ontology enrichment analysis revealed that differentially expressed genes were predominantly enriched in biological processes, molecular functions, cellular components, and the hematopoietic cell lineage pathway. A sepsis risk model constructed using five key genes—*CD8A, ITGAM, CXCL8, CCL5*, and *LCK*—demonstrated high predictive accuracy. Notable differences in immune cell composition were observed, with a statistically significant variation in T cells CD4 naïve and activated dendritic cells between the sepsis and control groups ($p < 0.05$). Additionally, a positive correlation was identified between *CXCL8* expression and the proportion of activated dendritic cells.

Conclusion: The severity of lung and kidney tissue damage in sepsis increased over time. The five identified sepsis-related genes have predictive value in assessing sepsis risk. Insights into the interactions between key genes and immune cell populations may contribute to improved clinical management of sepsis.

Keywords: GEO, immune cell infiltration, key genes, nomogram, sepsis

Introduction

Sepsis is a complex and heterogeneous syndrome resulting from microbial infection, which can lead to systemic complications of varying severity, including hypotension, organ failure, and shock.[1,2] According to a study, sepsis accounted for 29.5% of intensive care unit (ICU) admissions and was present in 18.0% of patients already receiving ICU care.[3] According to the Global Burden of Disease Study, an estimated 48.9 million new cases of sepsis occurred worldwide in 2017, with approximately 11 million sepsis-related deaths, representing 19.7% of total global mortality. The high morbidity and mortality associated with sepsis, along with the long-term functional impairment experienced by survivors, impose a significant burden on healthcare systems, society, and families.[4]

Received: 27 March 2025
Accepted: 8 August 2025
Published: 22 August 2025

In China, the incidence of sepsis remains a critical concern, particularly due to the increasing prevalence of chronic diseases, an aging population and advancements in medical technology.[5,6] The risk of sepsis is notably higher among patients with compromised immune function, including those with malignancies, severe immunodeficiency, and chronic kidney disease requiring hemodialysis. In the United States, more than 20% of adults hospitalized for sepsis have an underlying cancer diagnosis, while patients undergoing long-term hemodialysis have an approximately 40-fold increased risk of developing sepsis.[7]

Despite significant advancements in medical science, sepsis remains a leading cause of morbidity and mortality worldwide.[8] Current therapeutic strategies, including antibiotic administration to eliminate pathogens and supportive care measures such as hemodynamic stabilization, nutritional support, and organ function management, have contributed to improved outcomes.[9] However, these approaches remain insufficient in fully optimizing the prognosis of patients with sepsis.[10] Over the past few years, immunotherapy has emerged as a promising area of research, attracting considerable attention as a potential treatment strategy.[11] To facilitate the development of novel therapeutic approaches, authors have focused on identifying biomarkers associated with sepsis, yielding significant findings.[12–14] Advances in bioinformatics have provided robust methodologies for biomarker screening in sepsis.[15] The objective of this study was to evaluate the extent of lung and kidney tissue damage using a rat sepsis model, identify key sepsis-related genes, establish a sepsis risk model through bioinformatics analyses, and characterize immune cell infiltration patterns. Our findings demonstrate that the severity of pulmonary and renal tissue damage exhibited a time-dependent increase in sepsis. Furthermore, the five identified sepsis-associated genes show potential as predictive biomarkers for sepsis risk assessment. These findings contribute to the early identification and treatment of sepsis.

Materials and Methods

Materials

A total of 18 healthy male Wistar rats, aged 8–10 weeks and weighing between 200 and 250 g, were selected from the Center of Animal Experiments at Xinjiang Medical University. Following an acclimatization period of one week on a standard rat chow diet, the experiment commenced. A 12-hour fasting period was observed before the experiment, during which access to water remained unrestricted. Gene expression profiles were retrieved from the Gene Expression Omnibus (GEO) database (https://www.ncbi.nlm.nih.gov/geo/).

Experimental Group and Control Group

The 18 rats were randomly assigned to two groups, with nine animals in each group. The experimental group underwent cecal ligation and puncture to establish a sepsis model.[16] Anesthesia was administered via intraperitoneal injection at a dose of 0.5 mL/100 g body weight, using a mixture of ketamine, diazepam, and atropine in equal volumes, diluted with normal saline. The rats were immobilized, shaved, and disinfected, with pre-sterilized instruments utilized throughout the procedure. A 2 cm midline abdominal incision was made to expose the cecum, which was ligated below the ileocecal valve and perforated twice with an 18-gauge needle. The cecum was then repositioned, and the abdominal cavity was closed using sutures. Postoperative care involved subcutaneous saline injection (20 mL/kg) and thermostatic support to mitigate the risk of shock. In the control group, the abdominal cavity was opened solely to separate the mesentery of the cecum, followed by closure of the abdomen, with unrestricted access to food after surgery. Specimens were collected from both groups at 12-, 24-, and 36-hours post-operation.

Animals were monitored for predefined humane endpoints every 6 hours, including inability to access water, 20% body weight loss from baseline, persistent lethargy or unresponsiveness to stimuli, dyspnea, or cyanosis. Euthanasia was performed at 12, 24, and 36 hours post-surgery using a two-step protocol conforming to American Veterinary Medical Association (AVMA) standards: initial anesthesia with a 5% isoflurane-oxygen mixture (1 L/min) in an induction chamber for 3 minutes, followed by secondary euthanasia via intraperitoneal injection of sodium pentobarbital (150 mg/kg). Death was confirmed by absence of heartbeat for >2 minutes, fixed and dilated pupils, and cervical dislocation as an auxiliary physical method.[17]

Histopathological Differences in Lung and Kidney Tissues Were Evaluated Using Hematoxylin and Eosin (HE) Staining

Fixed lung and kidney tissue samples were rinsed under running water, dehydrated through a graded ethanol series, embedded in paraffin blocks, and sectioned into paraffin slices. The sections were sequentially stained with hematoxylin solution (Baso Diagnostics Inc., Zhuhai, BA-4041) for 3–5 minutes, followed by eosin solution (Baso Diagnostics Inc., Zhuhai, C0163M) for 5 minutes. Subsequently, the sections underwent a series of clearing steps, including immersion in absolute ethanol I (Tianjin Yongda Chemical Reagent Co., Ltd.) for 5 minutes, absolute ethanol II for 5 minutes, and absolute ethanol III for 5 minutes, followed by xylene I (Tianjin Yongda Chemical Reagent Co., Ltd.) for 5 minutes and xylene II for 5 minutes. Mounting was performed using neutral balsam (Beijing Zhongshan Jinqiao Biotechnology Co., Ltd., Zli-9555). Finally, the slides were examined under an optical microscope (BX43, Olympus, Japan), and target areas were selected for imaging.

Data Download and Processing

As illustrated in Supplementary Figure 1, the research workflow commenced with the establishment of an animal model and the acquisition of gene expression data from the GEO database. The GSE5706 gene expression profile was obtained from the GEO database (https://www.ncbi.nlm.nih.gov/geo/query/acc.cgi?acc). The expression profile data for the GSE25066 dataset was extracted using GPL570 [HG-U133]. This dataset includes data from 82 patients diagnosed with sepsis and 25 healthy controls, incorporating variables such as patient age, gender, sepsis status, collection time, and extracted molecular data. A total of 823 differentially expressed genes (DEGs) were identified through R-based processing, with high- and low-expression genes screened based on a threshold of $|\log FC| \geq 1$. Heatmaps and volcano plots were subsequently generated to visualize the expression patterns.

Statistical Analysis

The limma package was used for quality control, preprocessing, and statistical analysis of the data. Data normalization was performed using the robust multi-array average method. Differential gene expression analysis was conducted using limma, with genes meeting the criteria of a false discovery rate < 0.05 and a $\log_2$ fold change ≥ 1 selected for further weighted gene co-expression network analysis (WGCNA).

WGCNA

WGCNA is a systems biology approach used to characterize gene association patterns across samples, enabling the identification of highly co-expressed gene sets and facilitating the discovery of potential biomarker genes or therapeutic targets.[18] In this study, network construction and visualization were performed using the WGCNA package in R software. A soft-thresholding parameter (β) was applied, with its value determined based on the lowest power at which the scale-free topology model fit reached 0.8. Clustering dendrograms were generated to visualize distinct modules, represented by different colors. Dynamic modules with high similarity were merged at a cut-off threshold of 0.6. Pearson's correlation analysis was conducted to identify the module most strongly associated with sepsis, and gene significance and module membership values were calculated. Sepsis-related key genes were screened using the criteria of GS > 0.5 and MM > 0.8. These genes were then intersected with DEGs to identify key genes with differential expression.

GO and KEGG Enrichment Analysis

Functional enrichment analysis was conducted using the clusterProfiler package in R. The biological functions and pathways associated with the identified differentially expressed key genes were examined through Gene Ontology (GO) and Kyoto Encyclopedia of Genes and Genomes (KEGG) analyses. A significance threshold of $p < 0.05$ was applied to determine statistically significant enrichment.

Protein-Protein Interaction (PPI) Network

PPI networks represent interactions among proteins that contribute to various biological processes, including signal transduction, gene expression regulation, energy and substance metabolism, and cell cycle control.[19] Systematic analysis of PPIs within biological systems is essential for elucidating protein functional mechanisms, understanding biological signaling responses, and identifying metabolic changes under disease conditions or specific physiological states. In this study, a PPI network was constructed using DEGs identified through the STRING interactome. A high-confidence interaction score threshold of 0.9 was applied to minimize false positive interactions. To identify key hub genes within the network, the cytoHubba plug-in in Cytoscape software was used, enabling the construction of a core gene (hub gene) network diagram.

ROC Curve Drawing and Nomogram Establishment

Following the identification of core genes, a receiver operating characteristic curve was generated to assess their predictive accuracy for sepsis incidence. An area under the curve (AUC) ≥ 0.7 was considered indicative of good predictive performance. The risk score for sepsis was calculated using the following formula:. Risk Score = Expression of Gene1 × Coefficient of Gene1 + Expression of Gene 2 × Coefficient of Gene2 + Expression of Gene N × Coefficient of Gene N. Based on the calculated risk values, a core gene nomogram was developed to predict sepsis risk, providing a visual representation for clinical risk assessment.

Immune Cell Infiltration

The CIBERSORT algorithm is a computational method used to analyze immune cell infiltration by estimating the relative proportions of various immune cell types based on gene expression data. In this study, the CIBERSORT algorithm was applied to calculate the immune cell infiltration content in each sample. The results were visualized using the "heatmap" function in R. Additionally, heatmaps were generated to depict interactions among immune cell populations, allowing for the identification of immune cells with strong correlations.

Immune Cell Differences and Correlation Analysis

The ggplot2 package in R was used to generate violin plots depicting the distribution of immune cell content in the sepsis and primary groups. A *t*-test was conducted to evaluate the statistical significance of differences between the two groups, with $p < 0.05$ considered indicative of a significant difference. Additionally, a correlation analysis was performed to assess the association between core gene expression and immune cell populations. The results were visualized, with $p < 0.05$ set as the threshold for statistical significance.

Results

Damage in Kidney and Lung Tissues in Rats with Sepsis

According to the HE staining results of lung tissue in the control group (Figure 1A–C), the overall lung structure remained intact, with no significant changes observed in the alveolar cavity or alveolar wall. Additionally, no substantial infiltration of inflammatory cells was detected in the lung interstitium. In contrast, in the sepsis group (Figure 1D–F), lung tissue damage was significantly more severe compared to the control group. The alveolar cavity exhibited progressive narrowing, and by 36 hours, several alveolar cavities had disappeared. Moreover, extensive infiltration of red blood cells and immune cells was evident in the lung interstitium, indicating that in the absence of therapeutic intervention, lung tissue damage and inflammatory responses in septic rats worsened progressively over time.

Similarly, HE staining of kidney tissue revealed that in the control group (Figure 2A–C), the renal tissue structure remained intact, with well-preserved and structurally defined glomeruli that maintained close adherence to the renal capsule. The renal tubular casts appeared normal, with well-preserved nuclear structures, and no significant inflammatory cell infiltration was observed. These features remained stable over time. In contrast, in the sepsis group (Figure 2D–F), renal tissue exhibited more pronounced damage than in the control group. The glomeruli displayed irregular shapes and signs of atrophy, with partial loss of renal capsule integrity. The renal tubules demonstrated necrotic changes, and

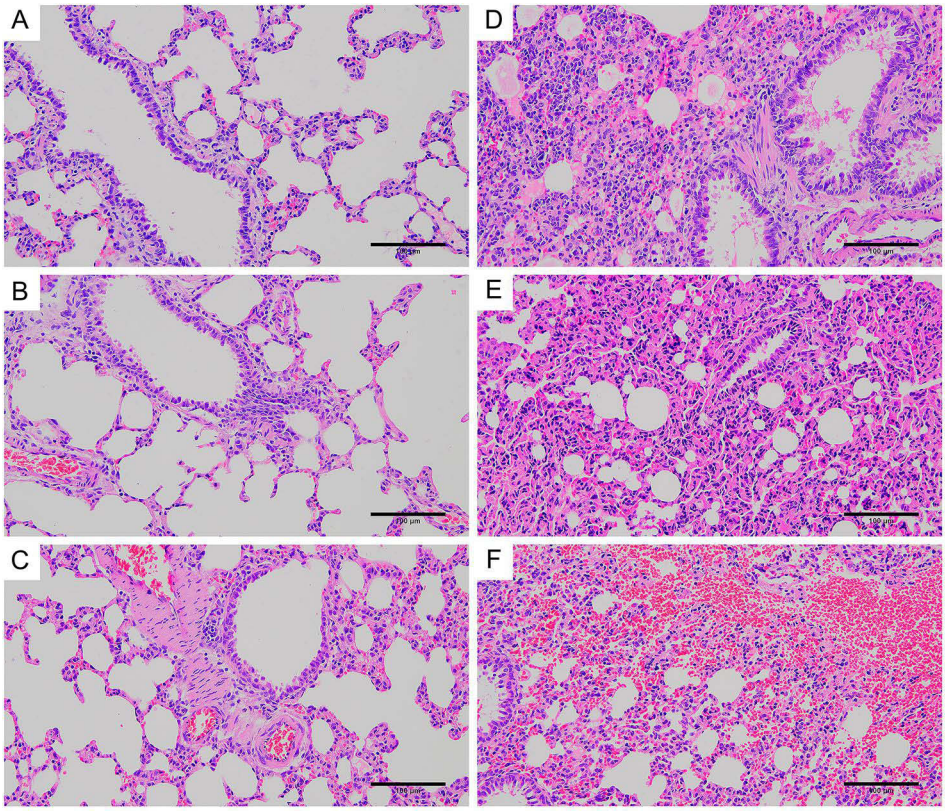

Figure 1 HE staining images of lung tissue (×200 times). (**A**) Lung tissue histology of rats in the primary group at 12 hours. (**B**) Lung tissue histology of rats in the primary group at 24 hours. (**C**) Lung tissue histology of rats in the primary group at 36 hours. (**D**) Lung tissue histology of rats in the sepsis group at 12 hours. (**E**) Lung tissue histology of rats in the sepsis group at 24 hours. (**F**) Lung tissue histology of rats in the sepsis group at 36 hours.

substantial inflammatory cell infiltration was observed in the glomerular and renal interstitial regions. These pathological changes became increasingly pronounced as time progressed.

DEGs in Patients with Sepsis

The sepsis-related gene expression data retrieved from the GEO database were processed and analyzed. Differential expression analysis was conducted between the normal and sepsis groups, applying the screening criteria of p-adjust < 0.05 and |logFC| ≥1. A volcano plot (Figure 3A) was generated to depict the distribution of DEGs. A total of 392 downregulated DEGs and 431 upregulated DEGs were identified. To further visualize the most significantly altered genes, a heatmap (Figure 3B) was generated, displaying the top 50 genes with the highest upregulated and downregulated expression levels.

Identification of the Most Relevant Gene Modules for Sepsis Using WGCNA

To further examine key genes associated with sepsis, WGCNA was conducted to identify the most relevant gene modules in sepsis samples. Based on scale independence and mean connectivity, a soft threshold of 4 was selected (Figure 4A). Using this threshold with the clustering dendrograms of these modules presented in Figure 4B and C, 20 modules were generated.

Additionally, the correlation between gene modules and sepsis was analyzed (Figure 4D). The blue module exhibited the strongest positive correlation with sepsis (4579 genes, r = −0.77, p = 7e−22), while the turquoise module demonstrated the highest negative correlation with sepsis (3346 genes, r = −0.89, p = 2e−38). Given this finding, the turquoise module was selected for further analysis. A strong association was also observed between module membership and gene importance within the turquoise module (r = 0.96, p < 1e−200) (Figure 4E), supporting its relevance for downstream investigations.

https://doi.org/10.2147/JIR.S530849

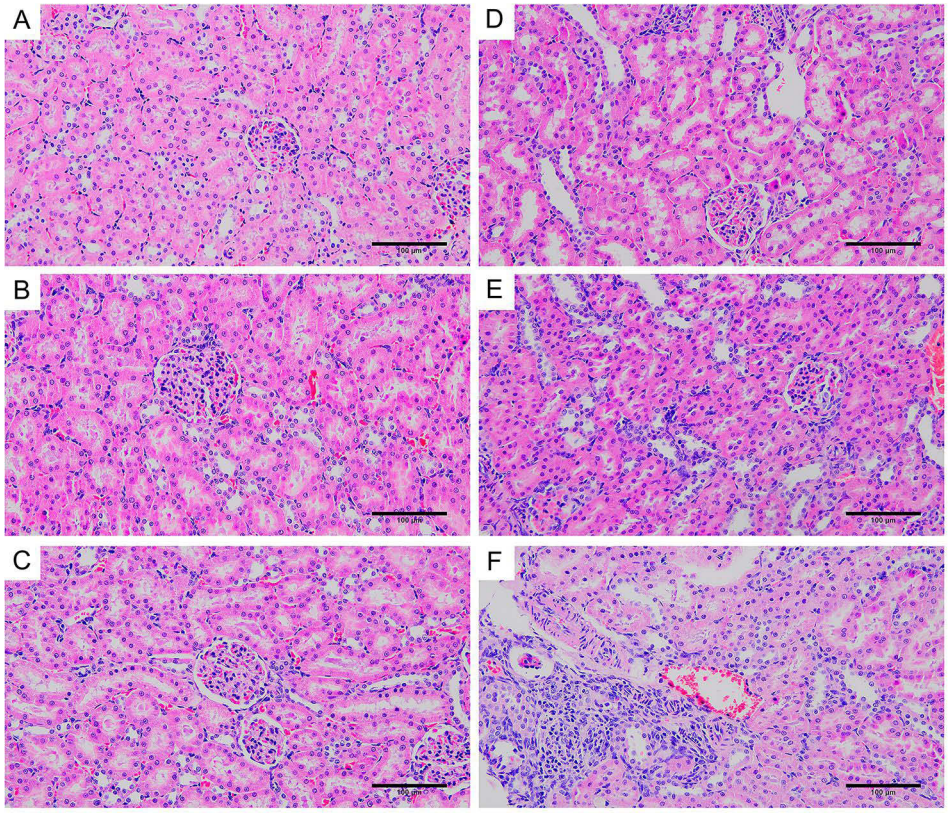

Figure 2 HE staining images of kidney tissue (×200 times). (**A**) Kidney tissue histology of rats in the primary group at 12 hours. (**B**) Kidney tissue histology of rats in the primary group at 24 hours. (**C**) Kidney tissue histology of rats in the primary group at 36 hours. (**D**) Kidney tissue histology of rats in the sepsis group at 12 hours. (**E**) Kidney tissue histology of rats in the sepsis group at 24 hours. (**F**) Kidney tissue histology of rats in the sepsis group at 36 hours.

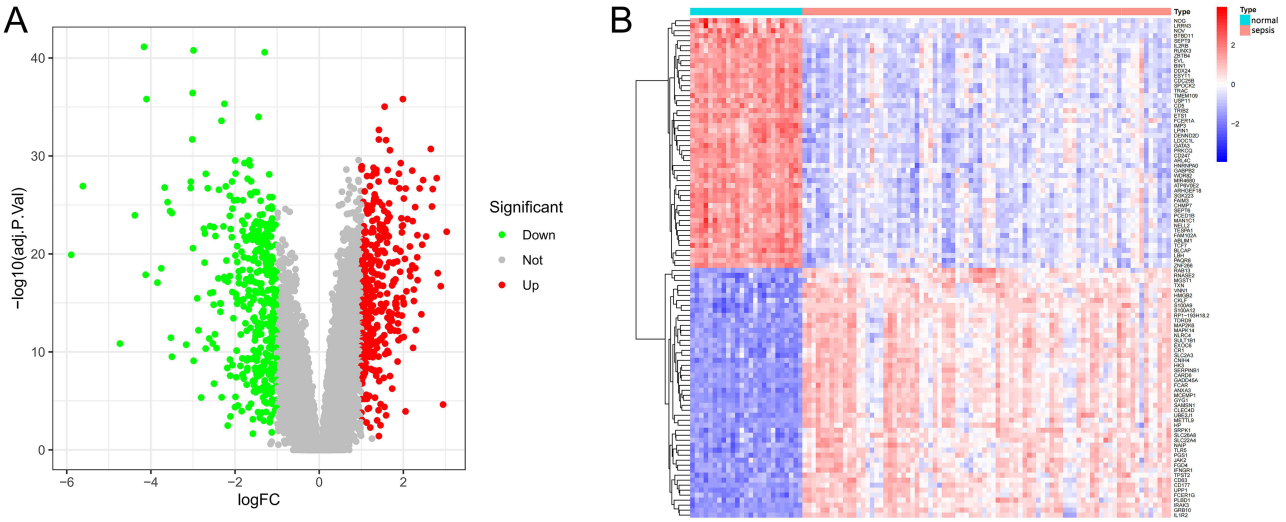

Figure 3 Volcano plot and heatmap of DEGs in sepsis and primary groups. (**A**) Volcano plot depicting DEGs in the sepsis dataset (upregulated genes are represented by red dots, while downregulated genes are represented by green dots). (**B**) Heatmap depicting the top 50 upregulated and top 50 downregulated DEGs in the integrated sepsis dataset.

Screening of Key Genes in Sepsis

A total of 3346 key genes in the turquoise module were identified as significantly associated with sepsis. To refine the selection of key genes implicated in sepsis onset, a cross-analysis was conducted between DEGs and WGCNA-identified key genes. Through this intersection, 505 key genes were identified for further analysis.

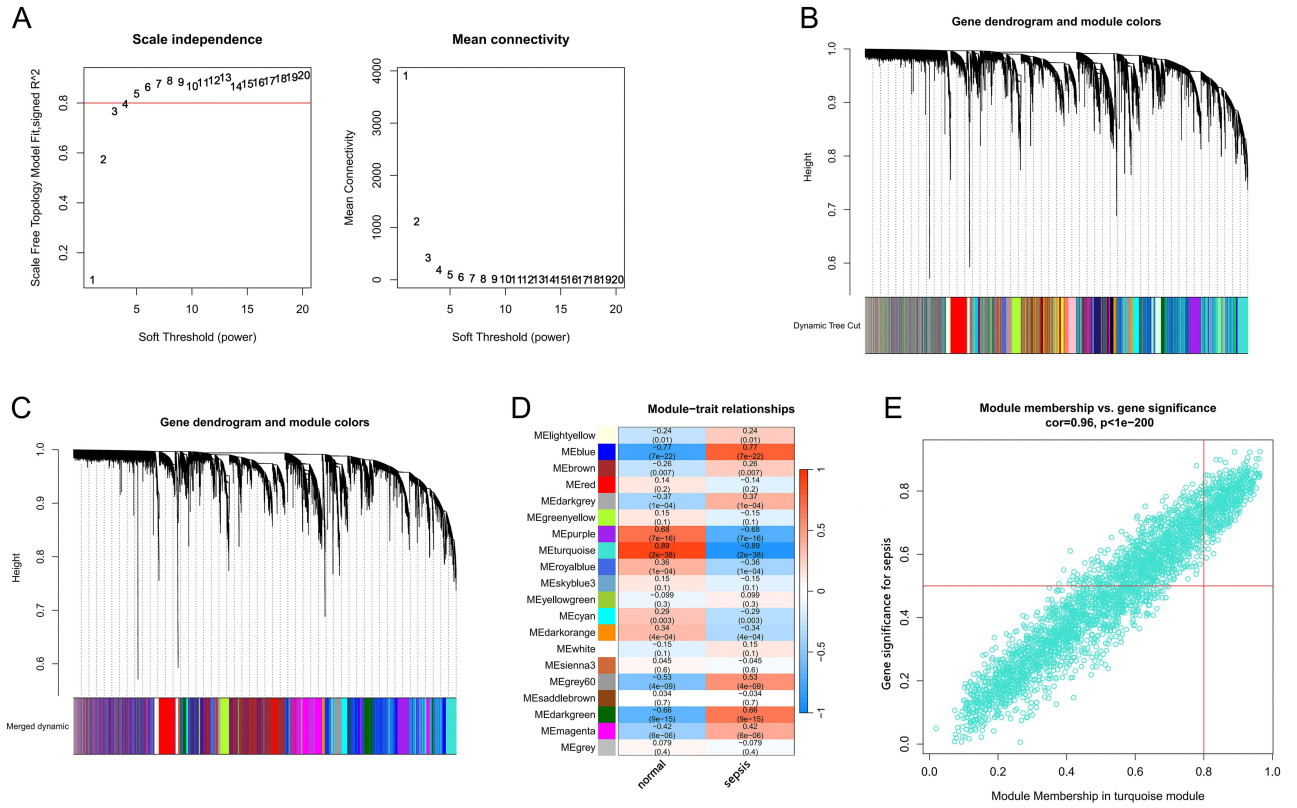

Figure 4 Identification of key gene modules associated with sepsis using WGCNA. (**A**) Determination of the optimal β value using the scale-free topology model, with β = 4 selected as the soft threshold based on mean connectivity and scale Independence. (**B** and **C**) Gene clustering dendrogram based on topological overlap, with assigned module colors. (**D**) Module-trait association matrix, where each row represents a module, and each column represents a clinical feature. Each cell contains the corresponding correlation coefficient and *p*-value, with the color gradient indicating the strength of the correlation. (**E**) Correlation analysis between module membership and gene significance in the turquoise module, depicting the relationship between module genes and sepsis-related traits.

GO and KEGG Enrichment Analysis

The biological functions of the identified differentially expressed key genes were examined through GO enrichment analysis, and the results were visualized using bubble diagrams (Figure 5A) and circle charts (Figure 5B). GO enrichment analysis revealed that the DEGs were primarily associated with biological processes (BP), molecular functions (MF), and cellular components (CC). In the BP category, enrichment was predominantly observed in leukocyte-mediated immunity. Within the MF category, the genes were mainly associated with immune receptor activity, while in the CC category, enrichment was observed in the secretory granule lumen.

Pathway analysis of the differentially expressed key genes was conducted using the KEGG analysis, and the results were visualized through bubble charts (Figure 5C) and bar charts (Figure 5D). KEGG enrichment analysis demonstrated that the DEGs in sepsis were primarily enriched in the hematopoietic cell lineage pathway.

Screening of Core Genes and Establishment of Nomogram

The STRING interactome was used to construct and visualize a PPI network from the filtered DEGs (Figure 6A). Through this analysis, core genes associated with sepsis pathogenesis were identified (Figure 6B). A total of five differentially expressed core genes—*CD8A, ITGAM, CXCL8, CCL5*, and *LCK*—were selected for further evaluation.

A nomogram for predicting the risk of sepsis onset was developed based on these core genes (Figure 6C), and the accuracy of the model was assessed using the ROC curve (Figure 6D). The risk score was calculated using the following formula: Risk Score = (0.214×*CD8A* Exp) + (0.208×*ITGAM* Exp) + (0.264×*CXCL8* Exp) + (0.325×*CCL5* Exp) + (0.285×*LCK* Exp). The AUC values for the core genes were as follows: *CD8A* (0.945), *ITGAM* (0.992), *CXCL8* (0.856), *CCL5* (0.944), and *LCK* (0.997). These results indicate that the nomogram demonstrated high accuracy in predicting sepsis risk.

https://doi.org/10.2147/JIR.S530849

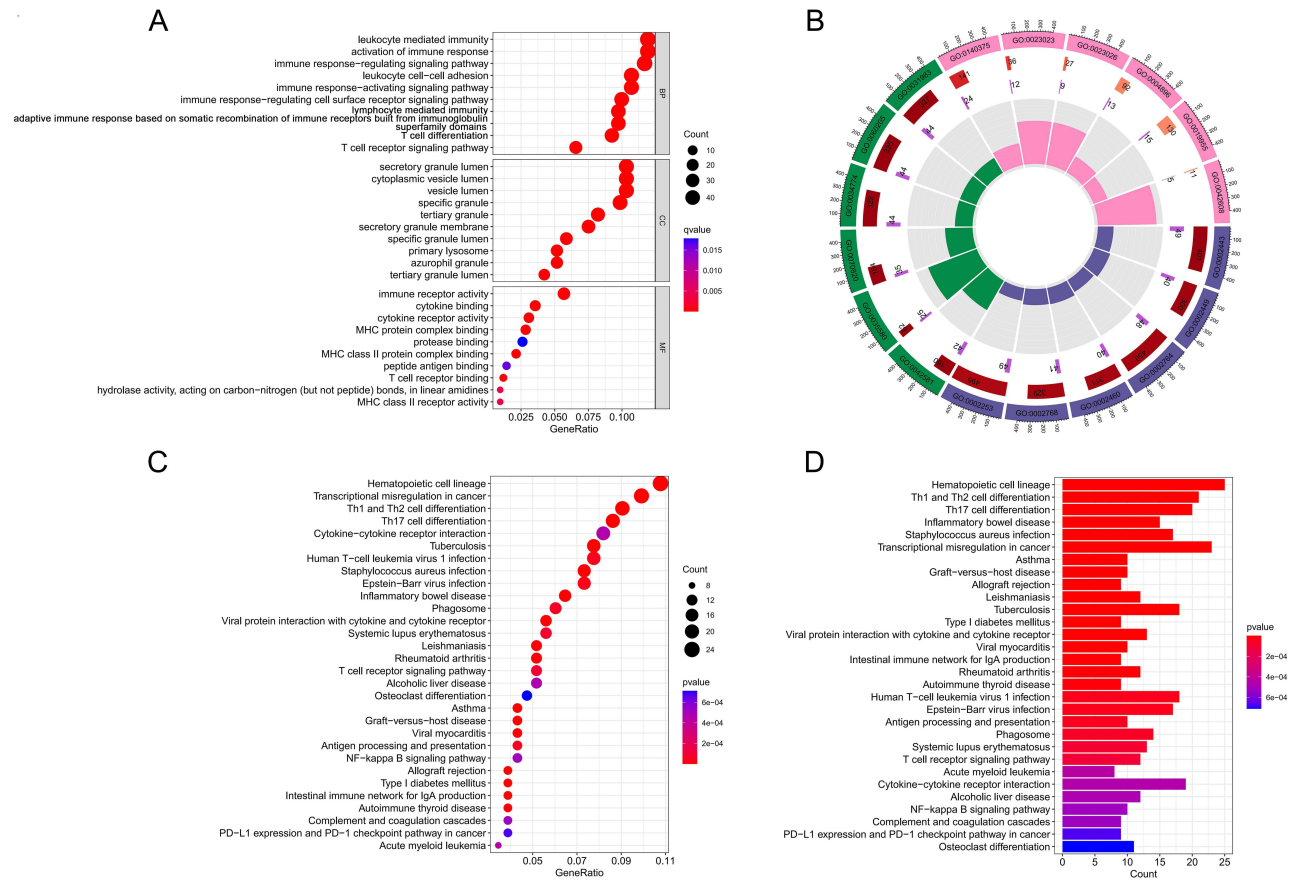

Figure 5 Functional enrichment analysis and immune-related functional analysis. (**A**) Bubble chart of GO enrichment analysis, depicting the BP, MF, and CC associated with differentially expressed key genes. (**B**) Circle chart of GO enrichment analysis, visualizing the functional categories of differentially expressed key genes. (**C**) Bubble diagram of KEGG enrichment analysis, revealing significantly enriched pathways related to sepsis. (**D**) Bar chart of KEGG enrichment analysis, highlighting key pathways associated with differentially expressed key genes in sepsis.

Immune Cell Content and Differential Analysis

A heatmap was generated to visualize the distribution of 22 types of immune cells in the normal and sepsis groups (Figure 7A). The analysis showed that activated CD4 memory T cells exhibited lower expression levels in sepsis samples, while activated dendritic cells displayed higher expression levels.

To further examine immune cell interactions, a correlation heatmap was constructed (Figure 7B). The results indicated a negative correlation between neutrophils and monocytes (correlation coefficient = −0.72) and a positive correlation between macrophages M1 and macrophages M0 (correlation coefficient = 0.62).

A violin plot was generated to compare the content of 22 immune cell types between the sepsis and primary groups (Figure 7C). *T*-tests were applied to identify immune cell types with significant differences in expression between the two groups. The results indicated that CD8 T cells (T cells CD8) ($p < 0.001$) and activated dendritic cells ($p = 0.042$) exhibited statistically significant differences in expression levels between the two groups.

Correlation Between Core Gene Expression and Immune Cell Expression

A lollipop chart was generated (Figure 8) to depict the correlation between core genes and immune cells. The analysis revealed the following associations:

CD8A expression (Figure 8A) exhibited a positive correlation with CD8 T cells (Cor = 0.71, $p < 0.001$) and a negative correlation with macrophages M0 (Cor = −0.53, $p < 0.001$).

ITGAM expression (Figure 8B) was positively correlated with naïve B cells (Cor = 0.26, $p = 0.017$) and negatively correlated with memory B cells (Cor = −0.26, $p = 0.016$).

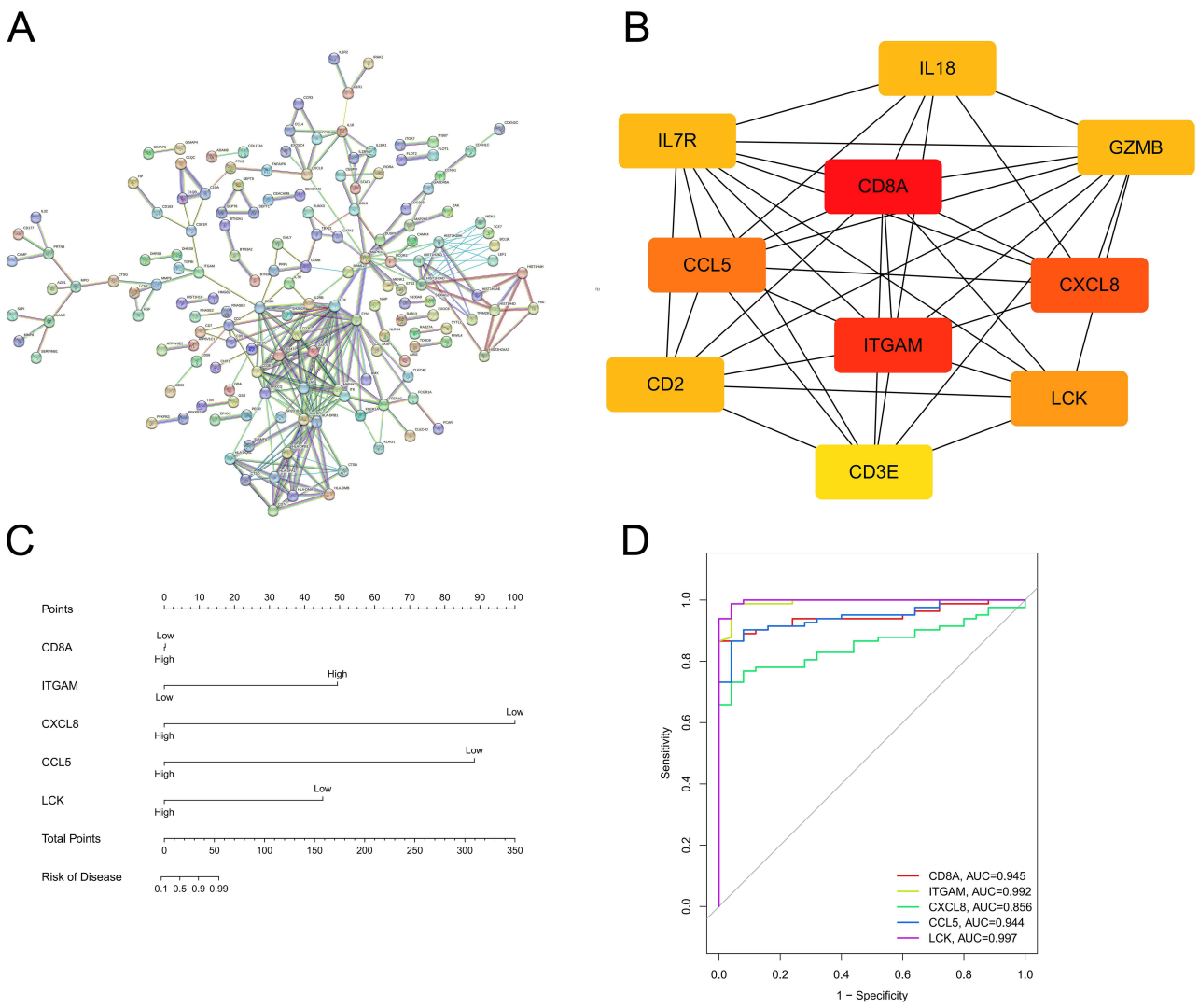

Figure 6 Screening of core genes and development of a nomogram. (**A**) PPI network of DEGs in sepsis. (**B**) Correlation network of the five core genes (*CD8A, ITGAM, CXCL8, CCL5*, and *LCK*) identified as key predictors of sepsis onset. (**C**) Nomogram for sepsis risk prediction, developed using core gene expression to estimate individual risk. (**D**) ROC curve, evaluating the predictive accuracy of each core gene included in the nomogram.

CXCL8 expression (Figure 8C) revealed a positive correlation with activated dendritic cells (Cor = 0.39, $p < 0.001$) and a negative correlation with plasma cells (Cor = −0.23, $p = 0.040$).

CCL5 expression (Figure 8D) was positively correlated with T cells CD8 (Cor = 0.62, $p < 0.001$) and negatively correlated with neutrophils (Cor = −0.38, $p < 0.001$).

LCK expression (Figure 8E) exhibited a positive correlation with T cells CD8 (Cor = 0.40, $p < 0.001$) and a negative correlation with macrophages M0 (Cor = −0.52, $p < 0.001$).

These findings highlight the significant interactions between core genes and immune cell populations in sepsis pathogenesis.

Discussion

Sepsis is a severe infectious disease frequently associated with multiple organ dysfunction and tissue damage.[20] Over the past few years, increasing attention has been directed toward the pathological mechanisms underlying tissue damage and immune cell infiltration in sepsis.[21–23] A more comprehensive understanding of the impact of sepsis on various organ

https://doi.org/10.2147/JIR.S530849

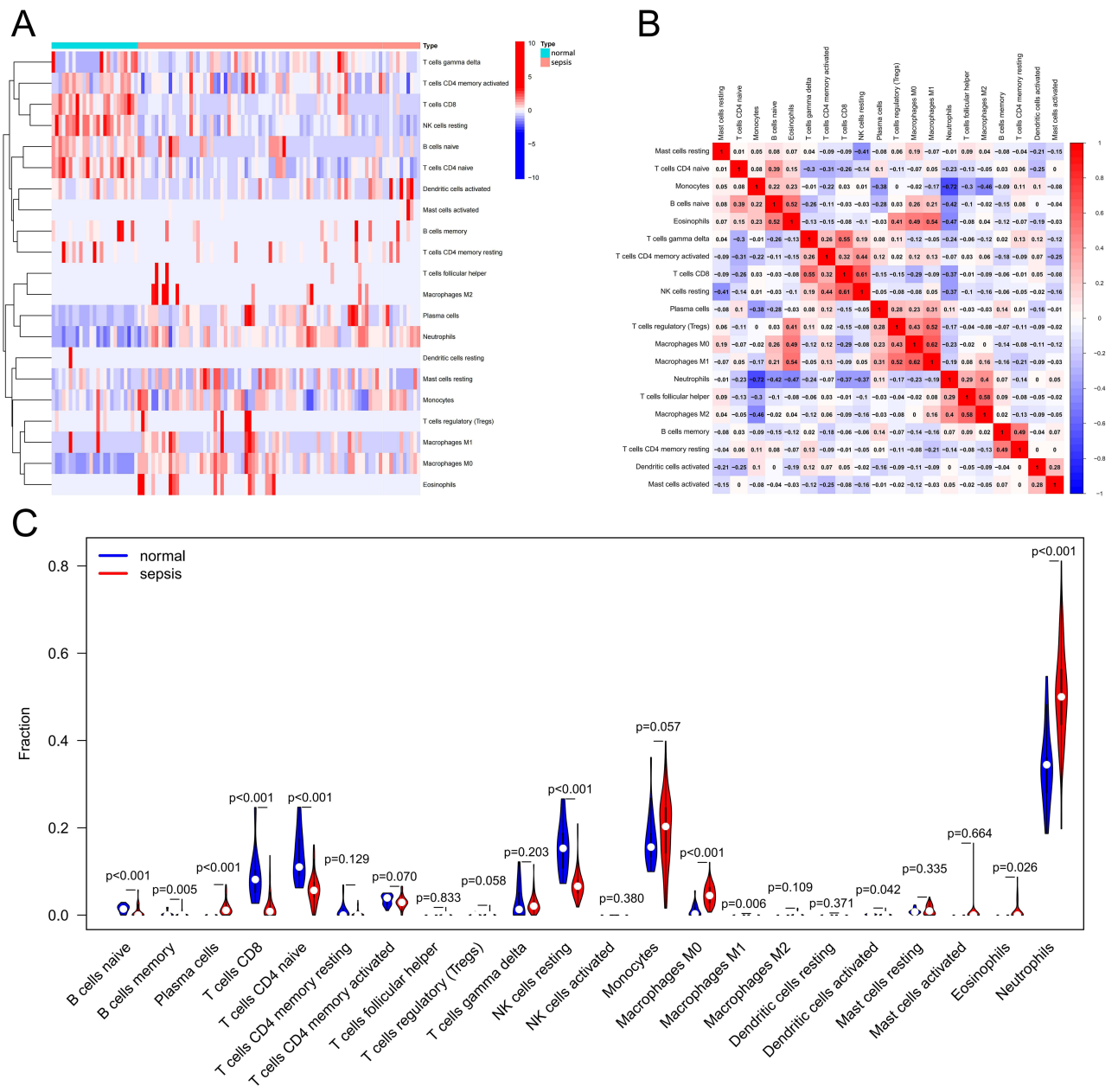

Figure 7 Immune cell composition, interactions, and differential analysis in sepsis. (**A**) Heatmap visualizing the distribution of immune cells in the sepsis and primary groups. (**B**) Heatmap of immune cell interactions in sepsis patients, illustrating correlation patterns among immune cell populations. (**C**) Violin plot depicting the comparative distribution of immune cell content between sepsis and primary groups, highlighting statistically significant differences.

systems can provide valuable insights into its pathogenesis and progression, thereby informing strategies for early diagnosis and targeted therapeutic interventions.

In this study, lung and kidney tissues in the sepsis group exhibited significant pathological damage compared to the control group, with the severity of tissue injury progressively increasing over time. These findings align with prior research, further supporting the notion that sepsis exerts extensive systemic effects and follows a dynamic progression.[24] Sepsis induces a robust inflammatory response, leading to an increased release of proinflammatory cytokines such as IL-1β, TNF-α, and IL-6, which promotes neutrophil infiltration and exacerbates lung tissue injury.[25] Additionally, Sepsis upregulates lung xanthine oxidase (XO) and malondialdehyde (MDA) via oxidative stress pathways, while suppressing superoxide dismutase (SOD) and glutathione peroxidase (GPx) activity, exacerbating oxidative tissue damage.[26]

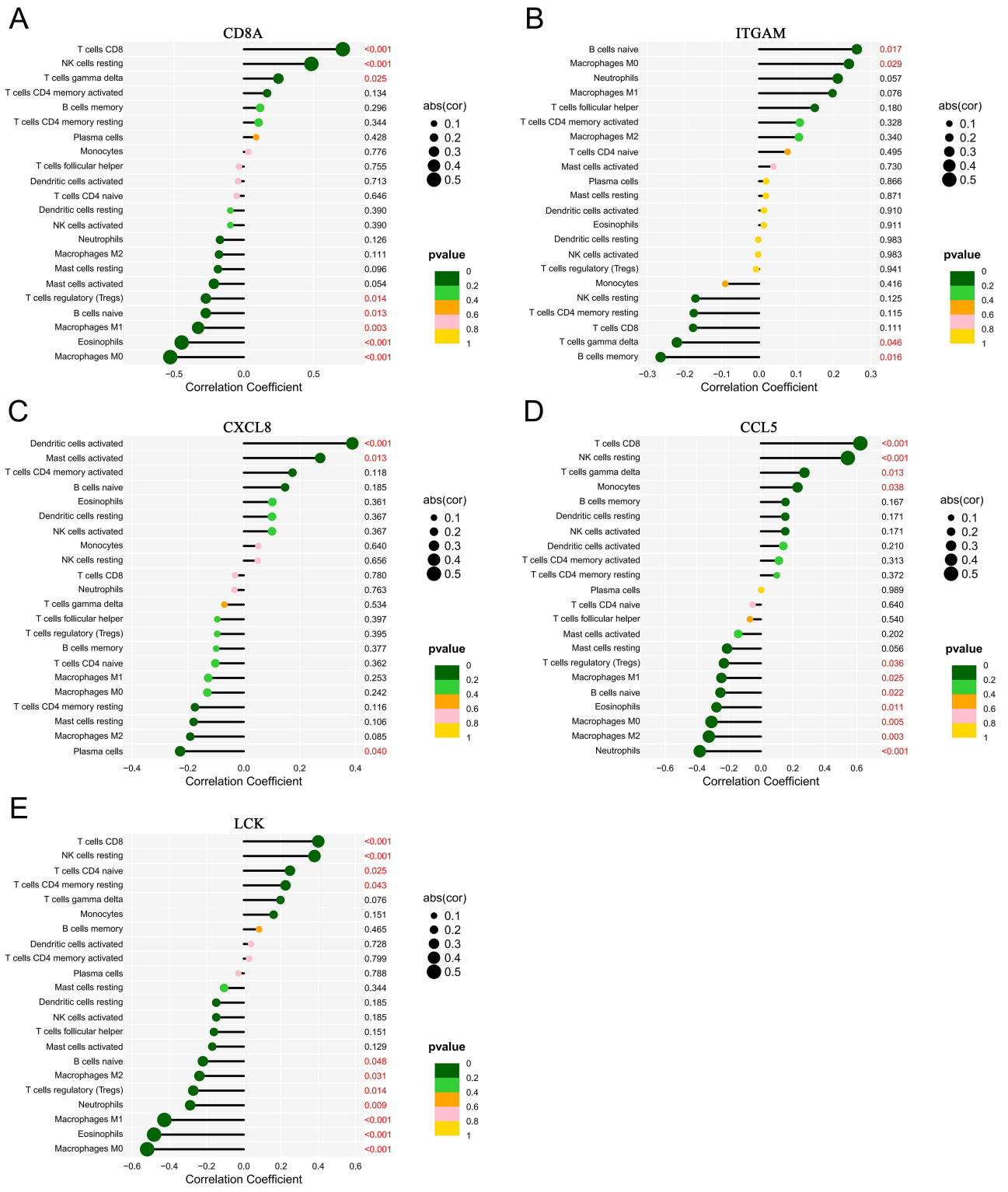

Figure 8 Lollipop chart depicting the correlation between core gene expression and immune cell populations. (**A**) Lollipop chart depicting the correlation between *CD8A* gene expression and various immune cell types. (**B**) Lollipop chart depicting the association between *ITGAM* gene expression and immune cell populations. (**C**) Lollipop chart revealing the correlation between *CXCL8* gene expression and immune cell infiltration. (**D**) Lollipop chart visualizing the relationship between *CCL5* gene expression and different immune cell subsets. (**E**) Lollipop chart representing the correlation between *LCK* gene expression and immune cell distribution.
Note: Numbers in red indicate statistically significant differences ($P < 0.05$).

https://doi.org/10.2147/JIR.S530849

Similarly, kidney tissue damage under septic conditions is characterized by inflammatory cell infiltration and swelling of renal tubular epithelial cells. These pathological changes are closely linked to impaired renal perfusion, tissue hypoxia, and reperfusion injury induced by sepsis.[27] Sepsis-associated renal vasoconstriction reduces glomerular blood flow and lowers the glomerular filtration rate, ultimately contributing to acute kidney injury.[28] Furthermore, ischemia-reperfusion injury affecting distal organs, including the liver and intestines, exacerbates renal damage indirectly through systemic inflammatory responses and oxidative stress pathways.[29]

Among the 20 gene modules identified through WGCNA, the turquoise module was the most representative module associated with sepsis, exhibiting a negative correlation with the condition. GO enrichment analysis indicated that DEGs in sepsis were primarily enriched in leukocyte-mediated immunity and molecular functions related to immune receptor activity. These findings provide important insights into the pathogenesis of sepsis, highlighting the role of leukocytes in immune defense mechanisms. Leukocytes play a key role in the immune response by mediating immune defense against infections.[30]

Prior studies demonstrated the significance of immune response pathways in disease progression. For instance, King et al investigated both animal models and human infection models, identifying that immune response pathway activation plays a pivotal role in dengue virus infection, with abnormal activation closely linked to disease severity.[31] Similarly, Li et al applied various analytical methods and observed that the immune response-regulating signaling pathway is significantly enriched in periodontitis, where it contributes to disease pathogenesis through immune cell activation and immune tolerance regulation.[32] Given these findings, a comprehensive investigation into leukocyte-mediated immunity and immune receptor activity in sepsis is essential for advancing understanding of the pathogenesis and developing novel therapeutic strategies.

Additionally, the cellular component analysis revealed that DEGs were predominantly enriched in the secretory granule lumen, while KEGG pathway analysis demonstrated significant enrichment in the hematopoietic cell lineage signaling pathway. These findings suggest that these pathways may play key roles in sepsis pathogenesis. Prior studies indicated that the secretory granule lumen pathway is closely associated with the development of inflammatory disorders, such as psoriasis and inflammatory bowel disease.[33] Furthermore, the hematopoietic cell lineage signaling pathway plays a key role in hematopoiesis, influencing the production and function of immune cells. Hematopoietic cell lineage differentiation contributes to the generation of lymphocytes, which are essential for adaptive immunity, as well as myeloid cells, which are key mediators of innate immunity and cytokine secretion for immune regulation.[34]

Given the involvement of these pathways in inflammatory diseases, further investigation into their functions offers new therapeutic targets and insights for the development of innovative treatment strategies for sepsis.

Through screening, *CD8A, ITGAM, CXCL8, CCL5*, and *LCK* were identified as key genes associated with the risk of sepsis onset. The identification of these genes provides potential diagnostic and therapeutic targets for sepsis.

CD8A encodes the CD8α chain, which functions as a co-receptor alongside the T cell receptor (TCR) in recognizing antigens presented by class I MHC molecules on the surface of antigen-presenting cells. This interaction initiates intracellular signal transduction pathways, leading to the activation of cytotoxic T lymphocytes, which subsequently produce lymphokines, facilitate cell adhesion and migration, and eliminate infected or malignant cells. *CD8A* has been implicated in the pathogenesis of various tumors and inflammatory diseases.[35–37]

The inflammatory and immune responses represent critical pathological mechanisms underlying ischemic stroke. *ITGAM* has been identified as a potential therapeutic target for ischemic stroke (IS), indicating a close association between *ITGAM* and immune regulation, thereby further supporting its role in sepsis pathogenesis.[38]

CXCL8, an important chemokine, plays a key role in inflammatory responses.[39,40] It is secreted by both immune and non-immune cells, including monocytes, macrophages, and endothelial cells, and mediates immune cell chemotaxis and activation by binding to chemokine receptors CXCR1 and CXCR2 on the cell surface. CXCL8 is involved in the initiation and maintenance of inflammation.[41]

As a chemokine, CCL5 recruits immune cells that express its receptor CCR5, thereby contributing to immune cell infiltration and migration.[42]

LCK is a key enzyme in TCR signal transduction. Upon TCR activation, LCK phosphorylates immunoreceptor tyrosine-based activation motifs in the cytoplasmic tail, triggering downstream signaling pathways involved in immune responses.[43]

In the complex pathogenesis of sepsis, abnormal expression of these genes significantly influences disease progression. Prior research demonstrated that immune-related genes play essential roles in sepsis onset and progression.[44] The key genes identified in this study also exhibit distinct expression patterns across different immune cell infiltration types. Further investigation into these genes enhances the understanding of the pathophysiological mechanisms of sepsis, providing a foundation for the development of new diagnostic and therapeutic strategies.

Correlation analysis between gene expression and immune cell infiltration revealed that CD8A expression was positively correlated with CD8 T cells and negatively correlated with macrophages M0. $CD8^+$ T cells eliminate pathogens by secreting cytokines and directly killing infected cells. Additionally, long-lived memory $CD8^+$ T cell populations provide enhanced protection against reinfection.[45]

During the early stages of inflammation, macrophages M0 recognize pathogen-associated molecular patterns and damage-associated molecular patterns released by pathogens or damaged tissues. These macrophages activate signaling pathways via pattern recognition receptors, thereby initiating inflammatory responses.[46,47] Inhibiting CD8A expression serves as a potential strategy to mitigate the inflammatory response in sepsis.

The expression of *ITGAM* exhibited a positive correlation with naïve B cells and a negative correlation with memory B cells. Naïve B cells serve as initiators of immune responses during inflammation. Upon encountering pathogens, these cells recognize T cell-dependent antigens via IgM receptors on their surface, leading to their activation, proliferation, and initiation of the immune response.[48] In contrast, memory B cells participate in granuloma formation and are capable of producing Th1 cytokines, such as IL-12 and IFN-γ. Additionally, memory B cells function as antigen-presenting cells, interacting with $CD4^+$ and $CD8^+$ T cells to enhance disease-specific cellular immune responses and contribute to immune protection.[49]

The expression levels of *CXCL8* and *LCK* were positively correlated with activated dendritic cells but negatively correlated with plasma cells. Dendritic cells are the most efficient antigen-presenting cells and become activated upon pathogen infection or other stimuli.[50] At inflammation sites, dendritic cells capture, process, and present pathogen-derived antigens to T and B cells, thereby initiating an adaptive immune response.[51] Whereas, plasma cells, which differentiate from B cells, function as antibody-secreting cells. These antibodies bind to pathogens, facilitating neutralization and clearance by phagocytes.[52]

CCL5 expression demonstrated a positive correlation with $CD8^+$ T cells and a negative correlation with neutrophils. Inflammatory responses involve the rapid migration of neutrophils to the site of infection through processes such as rolling, adhesion, crawling, and chemotactic migration, thereby exerting an anti-inflammatory effect.[53] The results indicate that CCL5 may regulate neutrophil function by influencing their migration, activation, or effector molecule release, although the underlying mechanism remains to be fully elucidated.

These findings highlight the complex interplay between key genes and immune cells, further elucidating the immune mechanisms underlying sepsis pathogenesis. Variations in the expression of key genes directly influence the function and abundance of immune cells, subsequently affecting sepsis progression.[54] Significant differences in the proportions of naïve B cells, memory B cells, plasma cells, $CD8^+$ T cells, and naïve $CD4^+$ T cells between the sepsis and primary groups were discovered in this study, which aligns with prior research.[55] Further investigation into the interactions between key genes and immune cells contributes to the development of new therapeutic strategies and enhances the effectiveness of sepsis treatment.

Despite the significant findings of this study, certain limitations should be acknowledged. The small sample size may not fully capture the multifactorial nature of sepsis pathogenesis, potentially introducing bias into the results. Future research should involve larger sample sizes to improve the reliability of findings, reduce sampling errors, and enhance statistical power. It should be noted that our experimental findings are derived from a rat sepsis model, whereas the bioinformatics analysis utilized human datasets. This cross-species approach may lead to potential discrepancies in future experimental validation.

Additionally, this study is primarily based on bioinformatics analysis, which, while valuable for identifying key genes and pathways, cannot fully replace experimental and clinical research. Future studies should incorporate experimental validation, including cell-based and animal studies, to further elucidate the functional mechanisms of the identified genes and pathways. Moreover, clinical research is necessary to evaluate the diagnostic and therapeutic relevance of these findings, ultimately contributing to a more comprehensive understanding of sepsis.

Conclusion

The severity of lung and kidney tissue damage in sepsis progressively increases over time. The five core sepsis-related genes—*CD8A, ITGAM, CXCL8, CCL5*, and *LCK*—identified through PPI network analysis and WGCNA demonstrate potential use in predicting the risk of sepsis onset. However, further research is required to elucidate the precise mechanisms underlying sepsis pathogenesis and to validate these findings through experimental and clinical studies.

Abbreviations

CLP, Cecal Ligation and Puncture; GEO, Gene Expression Omnibus; HE, Hematoxylin and Eosin; DEGs, Differentially Expressed Genes; WGCNA, Weighted Gene Co-expression Network Analysis; PPI, Protein - Protein Interaction.

Data Sharing Statement

The datasets used and analyzed during the current study are available from the corresponding author (Zhao-Xia Yu) upon reasonable request and GEO database (https://www.ncbi.nlm.nih.gov/).

Ethics Approval and Consent to Participate

All experimental procedures involving rats were strictly conducted in accordance with the ARRIVE guidelines 2.0 (Animal Research: Reporting of In Vivo Experiments). All experiments were evaluated and approved by the Ethics Committee of First Affiliated Hospital of Xinjiang Medical University (Approval No.: 20200320-88) and complied with the National Institutes of Health Guide for the Care and Use of Laboratory Animals.

This study qualifies for exemption from ethical review under Article 32 of the Measures for Ethical Review of Life Science and Medical Research Involving Human Subjects (2023), and was granted approval by the Ethics Committee of the First Affiliated Hospital of Xinjiang Medical University (Approval No.: 241015-01).

Acknowledgments

We want to acknowledge the hard and dedicated work of all the staff who implemented the intervention and evaluation components of the study.

Funding

Natural Science Youth Research Project of Xinjiang Medical University (2024XYZR50); 2023 “Youth Research Start” Special Fund Project (2023YFY-QKQN-41); General Project of the Natural Science Foundation of Xinjiang Uygur Autonomous Region (2023D01C100); “Tianshan Talent” High - level Talent Training Program of the Health Commission of Xinjiang Uygur Autonomous Region (TSYC202301A039); Outstanding Talent Training Project of the First Affiliated Hospital of Xinjiang Medical University (zyrc202401); The Natural Science Foundation of Xinjiang (Grant No. 2020D01C233).

Disclosure

The authors declare no conflicts of interest in this work.

References

1. Cecconi M, Evans L, Levy M, Rhodes A. Sepsis and septic shock. *Lancet*. 2018;392(10141):75–87. PMID: 29937192. doi:10.1016/S0140-6736(18)30696-2
2. Kellum JA, Formeck CL, Kernan KF, Gómez H, Carcillo JA. Subtypes and mimics of sepsis. *Crit Care Clin*. 2022;38(2):195–211. PMID: 35369943. doi:10.1016/j.ccc.2021.11.013
3. Vincent JL, Marshall JC, Namendys-Silva SA, et al; ICON Investigators. Assessment of the worldwide burden of critical illness: the intensive care over nations (ICON) audit. *Lancet Respir Med*. 2014;2(5):380–386. PMID: 24740011. doi:10.1016/S2213-2600(14)70061-X
4. Fleischmann-Struzek C, Rudd K. Challenges of assessing the burden of sepsis. *Med Klin Intensivmed Notfmed*. 2023;118(Suppl 2):68–74. PMID: 37975898; PMCID: PMC10733211. doi:10.1007/s00063-023-01088-7
5. Weng L, Xu Y, Yin P, et al; China Critical Care Clinical Trials Group (CCCCTG). National incidence and mortality of hospitalized sepsis in China. *Crit Care*. 2023;27(1):84. PMID: 36870989; PMCID: PMC9985297. doi:10.1186/s13054-023-04385-x
6. Levy MM. Identifying the burden of sepsis with big data. *Crit Care Med*. 2020;48(3):422–423. PMID: 32058377. doi:10.1097/CCM.0000000000004229

7. Meyer NJ, Prescott HC. Sepsis and Septic Shock. *N Engl J Med*. 2024;391(22):2133–2146. PMID: 39774315. doi:10.1056/NEJMra2403213
8. Markwart R, Saito H, Harder T, et al. Epidemiology and burden of sepsis acquired in hospitals and intensive care units: a systematic review and meta-analysis. *Intensive Care Med*. 2020;46(8):1536–1551. PMID: 32591853; PMCID: PMC7381455. doi:10.1007/s00134-020-06106-2
9. Prescott HC, Angus DC. Enhancing recovery from sepsis: a review. *JAMA*. 2018;319(1):62–75. doi:10.1001/jama.2017.17687
10. Giamarellos-Bourboulis EJ, Aschenbrenner AC, Bauer M, et al. The pathophysiology of sepsis and precision-medicine-based immunotherapy. *Nat Immunol*. 2024;25(1):19–28. PMID: 38168953. doi:10.1038/s41590-023-01660-5
11. Borouchaki A, de Roquetaillade C, Barthélémy R, Mebazaa A, Chousterman BG. Immunotherapy to treat sepsis induced-immunosuppression: immune eligibility or outcome criteria, a systematic review. *J Crit Care*. 2022;72:154137. doi:10.1016/j.jcrc.2022.154137
12. Pierrakos C, Velissaris D, Bisdorff M, Marshall JC, Vincent JL. Biomarkers of sepsis: time for a reappraisal. *Crit Care*. 2020;24(1):287. PMID: 32503670; PMCID: PMC7273821. doi:10.1186/s13054-020-02993-5
13. Barichello T, Generoso JS, Singer M, Dal-Pizzol F. Biomarkers for sepsis: more than just fever and leukocytosis-a narrative review. *Crit Care*. 2022;26(1):14. PMID: 34991675; PMCID: PMC8740483. doi:10.1186/s13054-021-03862-5
14. Póvoa P, Coelho L, Dal-Pizzol F, et al. How to use biomarkers of infection or sepsis at the bedside: guide to clinicians. *Intensive Care Med*. 2023;49(2):142–153. PMID: 36592205; PMCID: PMC9807102. doi:10.1007/s00134-022-06956-y
15. Peng Y, Wu Q, Liu H, et al. An immune-related gene signature predicts the 28-day mortality in patients with sepsis. *Front Immunol*. 2023;14:1152117. PMID: 37033939; PMCID: PMC10076848. doi:10.3389/fimmu.2023.1152117
16. Dejager L, Pinheiro I, Dejonckheere E, Libert C. Cecal ligation and puncture: the gold standard model for polymicrobial sepsis? *Trends Microbiol*. 2011;19(4):198–208. doi:10.1016/j.tim.2011.01.001
17. Percie du Sert N, Hurst V, Ahluwalia A, et al. The ARRIVE guidelines 2.0: updated guidelines for reporting animal research. *PLoS Biol*. 2020;18(7):e3000410. doi:10.1371/journal.pbio.3000410
18. Langfelder P, Horvath S. WGCNA: an R package for weighted correlation network analysis. *BMC Bioinf*. 2008;9:559. doi:10.1186/1471-2105-9-559
19. Majeed A, Mukhtar S. Protein-protein interaction network exploration using cytoscape. *Methods Mol Biol*. 2023;2690:419–427. doi:10.1007/978-1-0716-3327-4_32
20. Carcillo JA, Shakoory B. Cytokine storm and sepsis-induced multiple organ dysfunction syndrome. *Adv Exp Med Biol*. 2024;1448:441–457. PMID: 39117832. doi:10.1007/978-3-031-59815-9_30
21. Wu D, Spencer CB, Ortoga L, Zhang H, Miao C. Histone lactylation-regulated METTL3 promotes ferroptosis via m6A-modification on ACSL4 in sepsis-associated lung injury. *Redox Biol*. 2024;74:103194. PMID: 38852200; PMCID: PMC11219935. doi:10.1016/j.redox.2024.103194
22. Dong L, Xie YL, Zhang RT, Hu QY. Models of sepsis-induced acute kidney injury. *Life Sci*. 2024;352:122873. PMID: 38950643. doi:10.1016/j.lfs.2024.122873
23. Zhang WY, Chen ZH, An XX, et al. Analysis and validation of diagnostic biomarkers and immune cell infiltration characteristics in pediatric sepsis by integrating bioinformatics and machine learning. *World J Pediatr*. 2023;19(11):1094–1103. PMID: 37115484; PMCID: PMC10533616. doi:10.1007/s12519-023-00717-7
24. Rahimi A, Soudi S, Vakilian S, Jamshidi-Adegani F, Sadeghizadeh M, Al-Hashmi S. Bacteriophage M13 modulates the sepsis-related inflammatory responses and organ damage in a Clp model. *Shock*. 2023;59(3):493–504. PMID: 36576361. doi:10.1097/SHK.0000000000002076
25. Rittirsch D, Flierl MA, Ward PA. Harmful molecular mechanisms in sepsis. *Nat Rev Immunol*. 2008;8(10):776–787. PMID: 18802444; PMCID: PMC2786961. doi:10.1038/nri2402
26. Kamel M, Ahmed SM, Abdelzaher W. The potential protective effect of modafinil in intestinal ischemic reperfusion-induced in rats. *Int Immunopharmacol*. 2020;88:106983. PMID: 33182022. doi:10.1016/j.intimp.2020.106983
27. Okazaki N, Iguchi N, Evans RG, et al. Beneficial effects of vasopressin compared with norepinephrine on renal perfusion, oxygenation, and function in experimental septic acute kidney injury. *Crit Care Med*. 2020;48(10):e951–e958. PMID: 32931198. doi:10.1097/CCM.0000000000004511
28. Kuwabara S, Goggins E, Okusa MD. The pathophysiology of sepsis-associated AKI. *Clin J Am Soc Nephrol*. 2022;17(7):1050–1069. PMID: 35764395; PMCID: PMC9269625. doi:10.2215/CJN.00850122
29. Naito H, Nojima T, Fujisaki N, et al. Therapeutic strategies for ischemia reperfusion injury in emergency medicine. *Acute Med Surg*. 2020;7(1):e501. PMID: 32431842; PMCID: PMC7231568. doi:10.1002/ams2.501
30. Wang J, Gurupalli HV, Stafford JL. Teleost leukocyte immune-type receptors. *Dev Comp Immunol*. 2023;147:104768. PMID: 37414235. doi:10.1016/j.dci.2023.104768
31. King CA, Wegman AD, Endy TP. Mobilization and activation of the innate immune response to dengue virus. *Front Cell Infect Microbiol*. 2020;10:574417. PMID: 33224897; PMCID: PMC7670994. doi:10.3389/fcimb.2020.574417
32. Tang L, Zhou H, Chen D, Xiang R, Tang J. Weighted gene coexpression network analysis identified IL2/STAT5 signaling pathway as an important determinant of peri-implantitis. *Comput Math Methods Med*. 2022;2022:4202823. PMID: 36193198; PMCID: PMC9525745. doi:10.1155/2022/4202823
33. Ding RL, Zheng Y, Bu J. Exploration of the biomarkers of comorbidity of psoriasis with inflammatory bowel disease and their association with immune infiltration. *Skin Res Technol*. 2023;29(12):e13536. PMID: 38115636; PMCID: PMC10730979. doi:10.1111/srt.13536
34. Lareau CA, Romagnani C, Ludwig LS. Editorial: lineage tracing, hematopoietic stem cell and immune cell dynamics. *Front Immunol*. 2022;13:1062415. PMID: 36330528; PMCID: PMC9623280. doi:10.3389/fimmu.2022.1062415
35. Du Y, Zuo L, Xiong Y, Wang X, Zou J, Xu H. CD8A is a promising biomarker associated with immunocytes infiltration in hyperoxia-induced bronchopulmonary dysplasia. *J Inflamm Res*. 2023;16:1653–1669. PMID: 37092130; PMCID: PMC10120826. doi:10.2147/JIR.S397491
36. Liu Z, Liu L, Weng S, et al. Machine learning-based integration develops an immune-derived lncRNA signature for improving outcomes in colorectal cancer. *Nat Commun*. 2022;13(1):816. PMID: 35145098; PMCID: PMC8831564. doi:10.1038/s41467-022-28421-6
37. Zheng Z, Guo Y, Huang X, et al. CD8A as a prognostic and immunotherapy predictive biomarker can be evaluated by MRI radiomics features in bladder cancer. *Cancers*. 2022;14(19):4866. PMID: 36230788; PMCID: PMC9564077. doi:10.3390/cancers14194866
38. Hou L, Li Z, Guo X, et al. ITGAM is a critical gene in ischemic stroke. *Aging*. 2024;16(8):6852–6867. PMID: 38637126; PMCID: PMC11087101. doi:10.18632/aging.205729
39. Park SE, Park K, Kim E, et al. CXCL5/CXCL8 induces neutrophilic inflammation in peri-implantitis. *J Periodontal Res*. 2024;59(4):698–711. PMID: 38699841. doi:10.1111/jre.13230

40. Baggiolini M. CXCL8 - the first chemokine. *Front Immunol*. 2015;6:285. PMID: 26106391; PMCID: PMC4459227. doi:10.3389/fimmu.2015.00285
41. Cambier S, Gouwy M, Proost P. The chemokines CXCL8 and CXCL12: molecular and functional properties, role in disease and efforts towards pharmacological intervention. *Cell Mol Immunol*. 2023;20(3):217–251. PMID: 36725964; PMCID: PMC9890491. doi:10.1038/s41423-023-00974-6
42. Barczak K, Drożdzik A, Bosiacki M, et al. CCL5's role in periodontal disease: a narrative review. *Int J Mol Sci*. 2023;24(24):17332. PMID: 38139161; PMCID: PMC10744061. doi:10.3390/ijms242417332
43. Keller B, Kfir-Erenfeld S, Matusewicz P, et al. Combined immunodeficiency caused by a novel nonsense mutation in LCK. *J Clin Immunol*. 2023;44(1):4. PMID: 38112969; PMCID: PMC10730691. doi:10.1007/s10875-023-01614-4
44. Sun Z, Hu Y, Qu J, Zhao Q, Gao H, Peng Z. Identification of apoptosis-immune-related gene signature and construction of diagnostic model for sepsis based on single-cell sequencing and bulk transcriptome analysis. *Front Genet*. 2024;15:1389630. PMID: 38894720; PMCID: PMC11183325. doi:10.3389/fgene.2024.1389630
45. Reina-Campos M, Scharping NE, Goldrath AW. CD8+ T cell metabolism in infection and cancer. *Nat Rev Immunol*. 2021;21(11):718–738. PMID: 33981085; PMCID: PMC8806153. doi:10.1038/s41577-021-00537-8
46. Orecchioni M, Ghosheh Y, Pramod AB, Ley K. Macrophage polarization: different gene signatures in M1(LPS+) vs. classically and M2(LPS-) vs. alternatively activated macrophages. *Front Immunol*. 2019;10:1084. Erratum in: Front Immunol. 2020;11:234. doi:10.3389/fimmu.2020.00234. PMID: 31178859; PMCID: PMC6543837. doi:10.3389/fimmu.2019.01084
47. Wynn TA, Vannella KM. Macrophages in tissue repair, regeneration, and fibrosis. *Immunity*. 2016;44(3):450–462. PMID: 26982353; PMCID: PMC4794754. doi:10.1016/j.immuni.2016.02.015
48. Weisel NM, Joachim SM, Smita S, et al. Surface phenotypes of naive and memory B cells in mouse and human tissues. *Nat Immunol*. 2022;23(1):135–145. PMID: 34937918; PMCID: PMC8712407. doi:10.1038/s41590-021-01078-x
49. Inoue T, Kurosaki T. Memory B cells. *Nat Rev Immunol*. 2024;24(1):5–17. PMID: 37400644. doi:10.1038/s41577-023-00897-3
50. Gardner A, de Mingo Pulido Á, Ruffell B. Dendritic cells and their role in immunotherapy. *Front Immunol*. 2020;11:924. PMID: 32508825; PMCID: PMC7253577. doi:10.3389/fimmu.2020.00924
51. Morante-Palacios O, Fondelli F, Ballestar E, Martínez-Cáceres EM. Tolerogenic dendritic cells in autoimmunity and inflammatory diseases. *Trends Immunol*. 2021;42(1):59–75. PMID: 33293219. doi:10.1016/j.it.2020.11.001
52. Wang AA, Gommerman JL, Rojas OL. Plasma cells: from cytokine production to regulation in experimental autoimmune encephalomyelitis. *J Mol Biol*. 2021;433(1):166655. PMID: 32976908. doi:10.1016/j.jmb.2020.09.014
53. Maier-Begandt D, Alonso-Gonzalez N, Klotz L, et al. Neutrophils-biology and diversity. *Nephrol Dial Transplant*. 2024;39(10):1551–1564. PMID: 38115607; PMCID: PMC11427074. doi:10.1093/ndt/gfad266
54. Gong T, Liu Y, Tian Z, et al. Identification of immune-related endoplasmic reticulum stress genes in sepsis using bioinformatics and machine learning. *Front Immunol*. 2022;13:995974. PMID: 36203606; PMCID: PMC9530749. doi:10.3389/fimmu.2022.995974
55. Fan J, Shi S, Qiu Y, Liu M, Shu Q. Analysis of signature genes and association with immune cells infiltration in pediatric septic shock. *Front Immunol*. 2022;13:1056750. Erratum in: Front Immunol. 2023;14:1241047. doi:10.3389/fimmu.2023.1241047. PMID: 36439140; PMCID: PMC9686439. doi:10.3389/fimmu.2022.1056750